Atomic Charges, Dipole Moments, and Fukui Functions Using the Hirshfeld Partitioning of the Electron Density

F. DE PROFT,[1] C. VAN ALSENOY,[2] A. PEETERS,[2] W. LANGENAEKER,[3] P. GEERLINGS[1]

[1]*Eenheid Algemene Chemie (ALGC), Free University of Brussels (VUB), Faculteit Wetenschappen, Pleinlaan 2, B-1050 Brussels, Belgium*
[2]*Department of Chemistry, University of Antwerp (UIA), Universiteitsplein 1, B-2610 Antwerpen, Belgium*
[3]*Department of Molecular Design and Chemoinformatics, Janssen Research Foundation, Turnhoutseweg 30, B-2340 Beerse, Belgium*

Abstract: In the Hirshfeld partitioning of the electron density, the molecular electron density is decomposed in atomic contributions, proportional to the weight of the isolated atom density in the promolecule density, constructed by superimposing the isolated atom electron densities placed on the positions the atoms have in the molecule. A maximal conservation of the information of the isolated atoms in the atoms-in-molecules is thereby secured. Atomic charges, atomic dipole moments, and Fukui functions resulting from the Hirshfeld partitioning of the electron density are computed for a large series of molecules. In a representative set of organic and hypervalent molecules, they are compared with other commonly used population analysis methods. The expected bond polarities are recovered, but the charges are much smaller compared to other methods. Condensed Fukui functions for a large number of molecules, undergoing an electrophilic or a nucleophilic attack, are computed and compared with the HOMO and LUMO densities, integrated over the Hirshfeld atoms in molecules.

© 2002 Wiley Periodicals, Inc.   J Comput Chem 23: 1198–1209, 2002

Introduction

Atomic charges are frequently used by chemists in the interpretation of structural and chemical reactivity data (for a review, see e.g. ref. 1). They highlight the importance of considering molecules as an assembly of atoms, a central concept in chemistry.[2,3] Because atomic charges do not correspond to any physical observable quantity and thus are not uniquely defined quantum mechanically, many different definitions have been proposed in the literature. They can roughly be divided into two main categories: orbital-based methods, and methods based on the electrostatic potential or the electron density. Among the orbital based definitions of atomic populations we mention the famous Mulliken population analysis method[4] and the density matrix based normal population analysis.[5–7] In the electrostatic potential-based population analysis schemes, the molecular charge distribution is determined as the assembly of atom centered monopoles that reproduce the quantum chemically calculated molecular electrostatic potential as closely as possible.[8,9] However, problems with this method can be encountered when charges are to be assigned to atoms that are embedded deeply in a molecule. Cioslowski has proposed a population analysis method based on the atomic polar tensor.[10] In Bader's atoms in molecules approach,[2] the molecule is divided in spatial regions defining the atom and the number of electrons in each region is determined. The atomic region around a certain nucleus or atomic basin Ω_A lies between all zero-flux surfaces surrounding the nucleus. This surface is mathematically defined as

$$\nabla \rho(\mathbf{r})\mathbf{n} = 0 \tag{1}$$

where n is the normal vector. The AIM (Atoms in Molecules) electron population of the atom A is then determined by integrating the electron density within the atomic basin

$$N_A = \int_{\Omega_A} \rho(\mathbf{r})d\mathbf{r} \tag{2}$$

A clear advantage of this approach is that it provides a way to recover the concept of an atom in a molecule. A disadvantage however is the computational cost of most of the current implementations of the three-dimensional integration of the electron density in the atomic basin, necessary to determine the atomic charge. Moreover, atomic charges determined from this methods tend to be of high magnitude.

In this contribution, we will study the charge distributions, atomic dipole moments and Fukui functions resulting from the Hirshfeld partitioning of the charge density.[1] [In the literature, the resulting charges are sometimes referred to as "stockholder" charges, due to the analogy of the atom in the molecule with the situation of different stockholders in a company; the gain or loss is directly proportional with the share of the stockholder in the company.]

The charge q_A of an atom A in a molecule

$$q_A = Z_A - \int \rho_A(\mathbf{r})d\mathbf{r} \qquad (3)$$

where Z_A is the atomic number of A and $\rho_A(\mathbf{r})$ the electron density of A in the molecule considered. This atomic electron density $\rho_A(\mathbf{r})$ is obtained by multiplying the molecular electron density $\rho(\mathbf{r})$ with a density based proportionality factor or weight factor $w_A(\mathbf{r})$, defined as the ratio of the isolated atom electron density of A, $\rho_A^0(\mathbf{r})$, and the density constructed from superimposing the isolated electron densities of the atoms present at their position in the molecule (the so-called promolecule density):

$$w_A(\mathbf{r}) = \frac{\rho_A^0(\mathbf{r})}{\sum_X \rho_X^0(\mathbf{r})} \qquad (4)$$

This approach is based on the idea to describe the molecule by dividing it into atoms and see how these atoms differ from the isolated atoms. In this sense, "the charge becomes an unambiguous property of the charge density, independent of the mathematical formalism used to derive this distribution."[11] The atoms in molecules resulting from this approach differ from Bader's atoms in the sense that the former have diffuse boundaries, whereas the boundaries of the latter are discrete. Also, the so-called Stewart atoms possess no discrete boundaries.[12,13]

Recently, Parr and Nalewajski used information theory to decompose the molecular electron density into atomic contributions.[3] They proved that when the maximal conservation of the information content of isolated atoms is imposed upon molecule formation, one recovers the Hirshfeld partitioning of the electron density.

Hirshfeld charges have received considerably less attention in the literature than other population analysis methods. Maslen and Spackman compared Hirshfeld and Bader charges for a large series of diatomic molecules.[14] In the majority of cases, the charges were found to be directly proportional to the electronegativity difference of the two atoms or to the dipole moment. Moreover, based upon the comparison of a large amount of atoms in different chemical environments, they concluded that the charges given by both of the

methods to partition the electron density were similar. Davidson and Chakravorty explored Hirshfeld charges and atomic moments at the Hartree–Fock level for a series of molecules and compared them with Mulliken and Löwdin charges, using the STO-3G, 6-311G**, and Dunning–Hay split valence basis set, concentrating, however, less on their interpretation.[15] Atomic charges derived from different methods, including Hirshfeld charges, were studied by Wiberg and Rablen at the Hartree–Fock level.[16] Next to an investigation of the basis set dependence of the different approaches, charges were computed for a series of hydrocarbons and some simple organic molecules, not containing second row atoms. Finally, the dipole moments generated by the different charges were compared with the SCF dipole moments. Due to the natural definition of atomic monopoles in the Bader and Hirshfeld approaches, these authors also concluded that these methods are promising for the reproduction of molecular dipole moments and electrostatic potentials. Hirshfeld charges were also used in subsequent studies of Wiberg and coworkers, for example, in the study of intramolecular interactions in carbanions[17] and in the study of the rotational barrier of thioformamide.[18]

Very recently, Van Alsenoy et al. systematically studied the parameters determining Hirshfeld charges.[19] It was concluded that they exhibit a very low basis set dependence, and that the effect of electron correlation is comparable to the effect on Mulliken, NPA, ChelpG, and APT charges, as established by De Proft, Martin, and Geerlings,[20] but that the effect is smaller in absolute value. In a subsequent article, these authors proposed a method to obtain atomic charges based on modified Voronoi polyhedra, yielding, however, charges of the same quality as the Hirshfeld charges.[21]

In this article, Hirshfeld charges and atomic moments are calculated and analyzed for a large series of molecules. Moreover, they are used for the first time on an elaborate basis in the calculation of a reactivity index central in so-called conceptual density functional theory, the Fukui function.

Computational Details

All geometries were fully optimized at the B3LYP[22],[23]/6-31G* level (B3LYP/6-31+G* level for the anions), and the electron densities were obtained at the same level using the Gaussian 98 program[24] (for a detailed account on the Pople type basis sets, see ref. 25). This density functional was shown to yield a good performance in the computation of atomic charges,[20,26] dipole moments,[20,26] infrared intensities,[20,26] electrostatic potentials,[26,27] Fukui functions,[26,27] ionization energies,[28,29] electron affinities,[27,29] electronegativities,[28,29] and hardnesses.[28,29] A more detailed and recent account on the use of DFT methods in the calculation of molecular properties can be found in ref. 30.

Hydrogen charges listed are the average of the charges of the different hydrogen atoms on a heavy atom. Atomic dipole moments were calculated at the QCISD level,[31] using Dunning's aug-cc-pVDZ basis set.[32,33] This methodology was preferred so as not to simultaneously test the performance of B3LYP in the calculation of atomic moments and draw conclusions on the magnitude of the latter.

For the sake of clarity, we now give full details about the numerical integration method used in our work to determine the Hirshfeld charges.

Using the weight factor $w_A(\mathbf{r})$ in eq. (4), the total molecular electron density $\rho(\mathbf{r})$ is written as:

$$\rho(\mathbf{r}) = \sum_A \frac{\rho_A^0(\mathbf{r})}{\sum_X \rho_X^0(\mathbf{r})} \rho(\mathbf{r}) \tag{5}$$

The number of electrons, N_A, attributed to atom A is then defined as

$$N_A = \int d\mathbf{r} \, \frac{\rho_A^0(\mathbf{r})}{\sum_X \rho_X^0(\mathbf{r})} \rho(\mathbf{r}) \tag{6}$$

Due to the complicated nature of the integrandum, N_A cannot be calculated analytically. A numerical procedure leads to

$$N_A = \sum_g W(\mathbf{r}_g) \frac{\rho_A^0(\mathbf{r}_g)}{\sum_X \rho_X^0(\mathbf{r}_g)} \rho(\mathbf{r}_g) \tag{7}$$

in which the sum runs over points $\mathbf{r}_g$ of the (molecular) grid, $W(\mathbf{r}_g)$ being the appropriate (molecular) weightfactor.

Because a molecular charge distribution has a complicated structure (a peak on every atom) the molecular grid is in general obtained as a superposition of atomic grids $(\mathbf{r}_g, W_B(\mathbf{r}_g))$ centered on the different atoms. The weight factors of the different atomic grids are combined using the procedure introduced by Becke,[34] based on Voronoi polyhedra.

$$W(\mathbf{r}_g) = W_B(\mathbf{r}_g) * W_{\text{Becke}}(\mathbf{r}_g) \tag{8}$$

We can, therefore, formally write

$$N_A = \sum_B^B \sum_g W_B(\mathbf{r}_g) * W_{\text{Becke}}(\mathbf{r}_g) \frac{\rho_A^0(\mathbf{r}_g)}{\sum_X \rho_X^0(\mathbf{r}_g)} \rho(\mathbf{r}_g) \tag{9}$$

For this study atomic grids were obtained by combining Euler–McLaurin[35] with Lebedev[36] grids for the radial and respective angular integration, respectively, as proposed by Gill et al.[37] As mentioned above, atomic weight factors are combined using Becke's procedure, taking into account the improvement proposed by Stratmann et al.[38]

The atomic densities used were calculated for the neutral atoms in their respective spectroscopic ground state using the same basissets as that used to describe the atom in the molecule.

For completeness, given a 1-particle density matrix P_{ij} in a certain basis, the electron density in a point $\mathbf{r}$ is given by

$$\rho(\mathbf{r}) = \sum_{ij} P_{ij} \chi_i(\mathbf{r}) \chi_j(\mathbf{r}) \tag{10}$$

Results and Discussion

Organic Molecules

Table 1 lists the Hirshfeld charges for a series of typical molecules, containing a wide diversity of organic functional groups. For comparison, charges obtained from other population analysis schemes are listed in the same table; these are the orbital based Mulliken[4] and NPA charges,[5–7] the electrostatic potential-based CHELPG charges,[9] the charges based on the atomic polar tensor (APT),[10] and Bader's topological charges (AIM).[2] A first remark that can be made upon comparison of the Hirshfeld charges with the other charge distributions is that the charge separation in the former is in the majority of cases smaller. A few exceptions can, however, be found, for example, in the series of hydrocarbons listed in Table 1. For the hydrocarbons, the Hirshfeld charges assign small negative values to the carbon atoms. The next entries in Table 1 are atomic charges for a number of oxygenated compounds. It can be observed that the Hirshfeld charge on the oxygen typically lies around -0.2. The largest oxygen charge is observed in the water molecule, carbonyl oxygen charges range from -0.207 (formaldehyde) to -0.318 for the acetamide, illustrating the resonance occurring in this molecule. The charges occurring for sp^3 hybridized oxygens typically lie around -0.16 to -0.18, the only exception being the oxygen atom in methanol. The charges on carbonyl carbons vary from 0.125 in formaldehyde to 0.212 in acetic acid. In methanol and dimethylether, chosen as prototypes of alcohols and ethers, the carbon atoms directly bonded to oxygen have low, in these cases even negative, atomic charges. All the other population analysis methods assign much more ionicity to the C—O bond: on average, the charges on the oxygen atoms range from -0.4 to -0.6 for all schemes except AIM. The topological charges in the majority of cases assign more than one electron to the oxygen atom. It is interesting to consider in somewhat more detail the case of CO. Only one method, CHELPG, gives a polarization C$^-$O$^+$ in accordance with the experimental dipole moment, pointing from the carbon atom to the oxygen and correctly predicted at the B3LYP/6-31G* level. The experimental dipole moment of 0.110 D suggest a small charge separation, which is only encountered for CHELPG and Hirshfeld. It is interesting to note the large charge separation for this molecule as predicted by the AIM method.

For the sulphur containing compounds, a negative charge is assigned to sulphur atom. The results for these molecules are, however, somewhat less uniform. All methods tend to agree upon the negative charge for the S atom in H$_2$S, but for dimethylthioether however, results differ. Also for NH$_3$, a large difference occurs between the charge separation predicted by the Hirshfeld charges and the other population analysis. For the organonitrogen compounds (the simplest amine, imine, and nitril compounds), the usual C$^+$N$^-$ polarization is recovered. In phosphine, the phosphorous atom bears a small positively charged, in accordance with the slightly higher electronegativity of hydrogen with respect to phosphorous. For the organophosphorous compounds, a C$^-$P$^+$ polarization is predicted (derived from the charges of the simplest phosphoalkane, alkene and alkyne. For the nitro-compounds, the usual and expected N$^+$O$^-$ charge separation is found, although, again, it is smaller than the separations predicted by the other methods.

Table 1. Stockholder Charges for a Series of Organic Molecules, as Compared to Other Population Analysis Methods (All Values in $|e|$). Hydrogen Charges Listed Are the Average of the Charges of the Different Hydrogen Atoms on a Heavy Atom.

Molecule	Atom	Stockholder	Mulliken	ChelpG	NPA	APT	AIM
CH_4	C	−0.129	−0.629	−0.373	−0.915	0.001	−0.073
	H	0.032	0.157	0.093	0.229	0.000	0.018
C_2H_6	C	−0.081	−0.433	−0.027	−0.676	0.107	−0.012
	H	0.027	0.144	0.009	0.225	−0.036	0.004
C_2H_4	C	−0.082	−0.285	−0.252	−0.428	−0.041	−0.079
	H	0.041	0.143	0.126	0.214	0.021	0.039
C_2H_2	C	−0.099	−0.188	−0.241	−0.240	−0.195	−0.171
	H	0.099	0.188	0.241	0.240	0.195	0.171
Cyclopropane	C	−0.073	−0.300	−0.203	−0.467	0.029	−0.060
	H	0.036	0.150	0.101	0.233	−0.015	0.030
Cyclobutane	C	−0.050	−0.270	−0.018	−0.455	0.101	−0.004
	H	0.025	0.135	0.009	0.228	−0.050	0.002
Cyclohexane	C	−0.045	−0.254	0.022	−0.460	0.119	0.015
	H	0.022	0.127	−0.011	0.230	−0.060	−0.008
Benzene	C	−0.041	−0.129	−0.084	−0.235	−0.014	0.036
	H	0.041	0.129	0.084	0.235	0.014	0.036
H_2O	O	−0.315	−0.774	−0.729	−0.934	−0.491	−1.093
	H	0.157	0.387	0.364	0.467	0.246	0.547
CH_3OH	O	−0.241	−0.605	−0.611	−0.744	−0.566	−1.072
	C	−0.007	−0.205	0.226	−0.305	0.522	0.491
	H(O)	0.160	0.390	0.393	0.467	0.236	0.541
	H(C)	0.030	0.140	−0.003	0.194	−0.064	0.014
CO	C	0.081	0.174	−0.011	0.505	0.223	1.222
	O	−0.081	−0.174	0.011	−0.505	−0.223	−1.222
CO_2	C	0.323	0.719	0.742	1.017	1.086	2.301
	O	−0.162	−0.360	−0.371	−0.509	−0.543	−1.151
H_2CO	O	−0.207	−0.323	−0.394	−0.494	−0.534	−1.114
	C	0.125	0.080	0.427	0.226	0.685	1.036
	H	0.041	0.121	−0.017	0.134	−0.075	0.039
CH_3CHO	C1	−0.080	−0.517	−0.254	−0.782	−0.107	−0.063
	H(C1)	0.047	0.176	0.077	0.137	0.017	0.046
	C2(O)	0.144	0.261	0.526	0.410	0.754	1.042
	O	−0.235	−0.374	−0.451	−0.520	−0.596	−1.144
	H	0.030	0.102	−0.053	0.252	−0.103	0.023
CH_3COCH_3	C	−0.086	−0.526	−0.356	−0.771	−0.104	−0.062
	C(O)	0.173	0.453	0.649	0.586	0.779	1.055
	O	−0.254	−0.426	−0.496	−0.540	−0.634	−1.162
	H	0.042	0.171	0.093	0.249	0.010	0.039
HCOOH	C	0.185	0.366	0.584	0.644	1.053	1.646
	H(C)	0.062	0.148	0.032	0.152	−0.008	0.087
	O1	−0.265	−0.404	−0.488	−0.585	−0.666	−1.115
	O2	−0.166	−0.519	−0.554	−0.706	−0.662	−1.197
	H(O2)	0.185	0.409	0.426	0.494	0.283	0.580
CH_3COOH	C1	−0.076	−0.515	−0.303	−0.784	−0.061	−0.019
	H(C1)	0.050	0.186	0.099	0.259	0.025	0.054
	C2	0.212	0.556	0.709	0.823	1.097	1.613
	O1	−0.284	−0.451	−0.529	−0.595	−0.687	−1.215
	O2	−0.181	−0.556	−0.582	−0.717	−0.700	−1.120
	H(O2)	0.180	0.408	0.409	0.496	0.276	0.579
CH_3OCH_3	C	−0.005	−0.192	0.105	−0.309	0.536	0.491
	O	−0.168	−0.443	−0.363	−0.564	−0.716	−1.080
	H(C)	0.030	0.138	0.025	0.197	−0.059	0.015
CH_3CONH_2	C1	−0.084	−0.530	−0.357	−0.769	−0.055	−0.043
	H(C1)	0.043	0.171	0.096	0.248	0.004	0.036
	C2	0.168	0.578	0.784	0.684	1.079	1.539
	O	−0.318	−0.495	−0.565	−0.621	−0.763	−1.218
	N	−0.149	−0.739	−0.949	−0.862	−0.701	−1.225

Table 1. (Continued)

Molecule	Atom	Stockholder	Mulliken	ChelpG	NPA	APT	AIM
	H(N)	0.127	0.336	0.400	0.412	0.213	0.419
NH_3	N	−0.286	−0.888	−1.001	−1.109	−0.405	−1.038
	H	0.095	0.296	0.334	0.370	0.135	0.346
CH_3NH_2	C	−0.044	−0.309	−0.385	−0.473	0.370	0.319
	H(C)	0.026	0.142	−0.045	0.208	−0.061	0.332
	N	−0.224	−0.705	−0.947	−0.891	−0.422	−1.012
	H(N)	0.095	0.294	0.348	0.369	0.117	0.339
CH_2NH	C	0.019	−0.114	0.267	−0.095	0.315	0.757
	H(C)	0.043	0.143	0.019	0.179	−0.021	0.041
	N	−0.208	−0.463	−0.648	−0.614	−0.410	−1.177
	H(N)	0.103	0.291	0.343	0.351	0.137	0.339
HCN	H	0.131	0.250	0.196	0.231	0.243	0.225
	C	0.047	0.109	0.145	0.077	−0.044	1.004
	N	−0.178	−0.358	−0.341	−0.309	−0.198	−1.229
PH_3	P	0.024	−0.092	−0.259	0.015	0.356	1.322
	H	−0.008	0.031	0.086	−0.005	−0.119	−0.441
CH_3PH_2	C	−0.120	−0.617	0.176	−0.978	−0.073	−0.570
	H(C)	0.039	0.176	−0.009	0.247	−0.009	0.104
	P	0.038	0.072	−0.354	0.291	0.407	1.386
	H(P)	−0.018	0.009	0.102	−0.027	−0.154	−0.460
CH_2PH	C	−0.109	−0.462	−0.179	−0.810	−0.133	−0.968
	H(C)	0.051	0.184	0.120	0.312	0.055	0.072
	P	0.027	0.120	−0.159	0.387	0.170	1.276
	H(P)	−0.021	−0.025	0.098	−0.051	−0.148	−0.452
HCP	H	0.087	0.192	0.227	0.251	0.201	0.159
	C	−0.122	−0.254	−0.288	−0.737	−0.228	−1.312
	P	0.034	0.062	0.061	0.486	0.027	1.153
HNO_2	H	0.155	0.341	0.153	0.353	0.118	0.408
	N	0.232	0.294	0.559	0.361	0.988	0.456
	O	−0.193	−0.318	−0.356	−0.357	−0.553	−0.432
CH_3NO_2	C	−0.018	−0.334	−0.305	−0.531	0.104	0.225
	H(C)	0.187	0.206	0.132	0.255	0.037	0.253
	N	0.257	0.454	0.726	0.511	0.962	0.436
	O	−0.210	−0.369	−0.409	−0.373	−0.587	−0.457
H2S	S	−0.128	−0.235	−0.319	−0.304	−0.057	−0.072
	H	0.064	0.118	0.160	0.152	0.029	0.036
CH_3SCH_3	C	−0.076	−0.578	−0.099	−0.827	0.104	−0.119
	H	0.041	0.178	0.076	0.241	−0.020	0.040
	S	−0.092	0.089	−0.257	0.210	−0.090	−0.003
HF	F	−0.229	−0.465	−0.415	−0.535	−0.359	−0.669
	H	0.229	0.465	0.415	0.535	0.359	0.669
CH_3F	C	0.027	−0.119	0.124	−0.183	0.603	0.541
	F	−0.144	−0.310	−0.230	−0.377	−0.455	−0.640
	H	0.039	0.143	0.035	0.186	−0.049	0.031
CF_4	C	0.342	0.950	0.594	1.413	2.002	2.497
	F	−0.085	−0.237	−0.148	−0.353	−0.500	−0.624
HCl	Cl	−0.137	−0.226	−0.237	−0.282	−0.191	−0.263
	H	0.137	0.226	0.237	0.282	0.191	0.263
CH_3Cl	C	−0.019	−0.518	−0.153	−0.650	0.316	0.067
	Cl	−0.137	−0.090	−0.177	−0.082	−0.289	−0.264
	H	0.052	0.202	0.110	0.244	−0.009	0.066
CCl_4	C	0.181	−0.358	−0.239	−0.270	1.477	0.392
	Cl	−0.045	0.089	0.060	0.068	−0.369	−0.098

Finally consider the halogenated compounds. As could be expected, the charge separation is C^+X^-, the magnitude decreasing when going from fluorine to chlorine. Also, in these cases, the charge transfer is much smaller within the Hirshfeld scheme than for the other methods, although the magnitudes become more comparable for molecules containing second-row
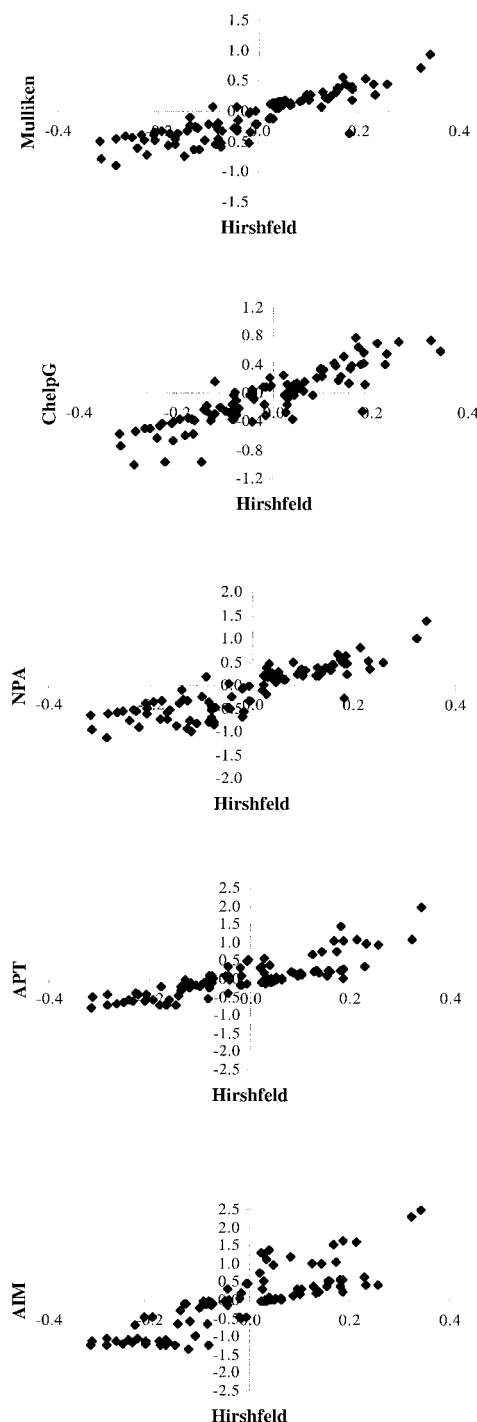
Figure 1. Correlation between the Hirshfeld charges and the Mulliken, NPA, ChelpG, APT and AIM charges, respectively, for the set of molecules considered in Table 1.

atoms. In Figure 1, the correlation of the Hirshfeld charges for these molecules with the other population analysis methods is given. As can be seen, the majority of points are located in the $(-,-)$ and $(+,+)$ quadrants of the graphs, the range being

much larger for the other population analysis methods, especially for the AIM charges.

Hypervalent Compounds

In this section, Hirshfeld charges calculated for some hypervalent compounds will be discussed. It is interesting to consider these compounds within the light of a debate in the literature about the role the d-orbitals in the bonding process taking place in these molecules. A thorough review about the situation in the literature has been given by Reed and Schleyer.[39] Basically two opposite views exist. Whereas it has been claimed that the d orbitals should be considered as valence orbitals, Reed and Schleyer argue that these have a polarization effect only, necessary to obtain good geometries. Moreover, they were found to have low orbital populations. The result is that large polarities exist in bonds such as the S—O bond and the P—O bond, a result confirmed by Cioslowski et al. based on APT charges. Table 2 lists the atomic charges using the same methods as in Table 1 for four prototype "hypervalent" molecules, $(CH_3)_2SO_2$, $(CH_3)_2SO$, SO_2Cl_2, and H_3PO. It can indeed be seen, as especially predicted by the NPA, APT, and AIM methods, that the S—O and P—O bonds are highly polar, in support of the view of Reed and Schleyer. The Hirshfeld charges for S lie between 0.271 in $(CH_3)_2SO$, one of the rare cases where it is higher than CHELPG, and 0.525 in SO_2Cl_2, whereas the charge on P in H_3PO is 0.384. When compared to Table 1, these are relatively high Hirshfeld charges (for comparison, the charge on hydrogen in HF is $+0.23$). To make a more objective statement about ionicity, we calculated the Hirshfeld charges for four ionic compounds LiF, NaF, LiCl, and NaCl. The charges on Li and Na are, respectively, (0.511), (0.484) and (0.533), (0.519). In view of these results, the hypervalent compounds can indeed be considered as somewhat ionic, in agreement with the statements of Reed and Schleyer. To make a more firm statement also about the involvement of d orbitals, it would be instructive to integrate the densities of the MOs having a high d orbital character over the Hirshfeld atoms in the molecule.

Atomic Dipoles

An additional property of the Hirshfeld atoms in molecules that merits further attention are their moments. The nth component of the dipole moment of atom i is

$$\mu_{i,n} = -\int r_n \Delta\rho_i(r) dr \tag{11}$$

where the atom is taken to be at the origin and where $\Delta\rho_i(r)$ is the deformation density of this atom, defined here as:

$$\Delta\rho_i(r) = \frac{\rho_i^0(r)}{\sum_X \rho_X^0(r)} \rho(r) - \rho_i^0(r) \tag{12}$$

One can thus prove that the n-component of the molecular dipole moment can exactly be written as:

Table 2. Stockholder Charges for a Selected Number of Hypervalent Compounds, as Compared to Other Population Analysis Methods (All Values in $|e|$).

Molecule	Atom	Stockholder	Mulliken	ChelpG	NPA	APT	AIM
$(CH_3)_2SO_2$	S	0.465	1.074	0.963	2.186	1.766	2.489
	O	−0.336	−0.528	−0.520	−0.955	0.772	−1.313
	C	−0.075	−0.630	−0.380	−0.932	−0.202	−0.155
$(CH_3)_2SO$	S	0.271	0.750	0.216	1.260	0.849	1.269
	O	−0.386	−0.625	−0.423	−0.957	−0.663	−1.249
	C	−0.087	−0.627	−0.181	−0.898	−0.117	−0.172
SO_2Cl_2	S	0.525	0.918	0.685	1.973	2.264	2.682
	O	−0.222	−0.398	−0.290	−0.812	−0.683	−1.198
	Cl	−0.040	−0.061	−0.052	−0.175	−0.449	−0.143
H_3PO	P	0.384	0.607	0.742	1.262	1.415	2.935
	O	−0.385	−0.552	−0.575	−1.019	−0.725	−1.429

$$\mu_n = \sum_i q_i R_{i,n} + \sum_i \mu_{i,n} \tag{13}$$

where $R_{i,n}$ is the nth component of the coordinates of atom i in the molecular coordinate system, and q_i the Hirshfeld charge on i.

The first term in this equation can be interpreted as the contribution to the dipole moment due to the charge transfer upon molecule formation, whereas the second term constitutes the intra-atomic charge polarization contribution. In Table 3, the contribution of both terms to the dipole moment is evaluated at the QCISD/aug-cc-pVDZ level. It thus represents the first calculation of these properties at the correlated level. Study of these properties is interesting for two reasons. First of all, it gives a measure of the possibility of the charges to reproduce the molecular dipole moment. Moreover, it was remarked by Hirshfeld that the atomic dipoles seem to be somewhat transferable between similar molecules. All molecules have been placed as such that the dipole moment is oriented along the z-axis in the positive direction; the origin was chosen to be the center of mass; planar molecules were positioned in the (x, z) plane. It is immediately clear that both terms are important in the correct description of the dipole moments. In the cases of BH, CO, and PH_3, for example, the sign of the dipole moment as derived from the charge transfer term differs from the sign of the molecular dipole moment. In BH, the dipole moment is mainly determined by the large atomic dipole moment of B. In CO, the small positive dipole moment (as correctly predicted by the QCISD method to correspond with a $C^{\delta-}$–$O^{\delta+}$ polarization) is caused by the near cancellation of the positive contribution of the atomic dipole of carbon caused by the non-bonding σ orbital on this atom and the negative contributions of the atomic dipole of O and the charge transfer term. In PH_3, it is mainly the atomic dipole of P that contributes to the dipole moment: the charge transfer terms are of opposite sign and are much smaller. The atomic dipoles seem to quantify the availability of lone pair electrons: consider, for example, the atomic dipole of N in NH_3 (0.231), which is larger than that on the P in PH_3 (0.168), in agreement with the lower basicity of the latter. The same can be concluded for H_2O and H_2S. An interesting last feature is also the relatively large atomic dipoles of acidic hydrogen atoms, as, for example, in HCN, HF, and HCl, the largest value (0.258) occurring

in HF. The link between the magnitudes of the atomic dipoles and various chemical properties should be investigated further. The analysis presented so far can be reconciled with earlier contributions, at the *ab initio* Hartree–Fock level, by two of the present authors concerning the importance of the hybridization and homopolar terms in dipole moments and their derivatives.[40–42]

Fukui Functions

In this section, Hirshfeld charges will be used to calculate the condensed Fukui functions. This function $f(\mathbf{r})$, introduced by Parr and Yang,[43] a generalization of Fukui's frontier MO reactivity index,[44] is an important property in the field of conceptual DFT, the section of DFT where response functions are identified with chemical properties that were readily used by chemists on, in most cases, a purely empirical basis.[45–47] It is introduced as[43]

$$f(\mathbf{r}) = \left(\frac{\partial \rho(\mathbf{r})}{\partial N} \right)_v \tag{14}$$

the derivative of the electron density with respect to the number of electrons. Due to the fact that the electron density is discontinuous with respect to the number of electrons, a left-hand and a right-hand side derivative are introduced as

$$f^+(\mathbf{r}) = \left(\frac{\partial \rho(\mathbf{r})}{\partial N} \right)_v^+ \tag{15}$$

$$f^-(\mathbf{r}) = \left(\frac{\partial \rho(\mathbf{r})}{\partial N} \right)_v^- \tag{16}$$

where f^+ can be used to probe the reactivity when electrons are added to the system (attack of a nucleophile) and f^- to probe the reactivity when electrons are extracted from the system (attack of an electrophile).

Within a finite difference approximation, (15) and (16) can be approximated as

$$f^+(\mathbf{r}) \approx \rho_{N+1}(\mathbf{r}) - \rho_N(\mathbf{r}) \tag{17}$$

Table 3. Atomic Dipoles and Charge Transfer Contributions, Together with the Total Dipole Moment for a Series of Small Molecules, Determined at the QCISD/aug-cc-pVDZ Level. (All Values are in a.u. For the orientation of the molecules, see text.)

Molecule	Atom	Atomic dipoles			Charge transfer			μ_Z
		x	y	z	x	y	z	
BH	B	0.000	0.000	0.656	0.000	0.000	−0.015	0.535
	H	0.000	0.000	0.058	0.000	0.000	−0.163	
HCN	H	0.000	0.000	0.188	0.000	0.000	0.379	1.186
	C	0.000	0.000	0.258	0.000	0.000	0.053	
	N	0.000	0.000	0.110	0.000	0.000	0.198	
CO	C	0.000	0.000	0.214	0.000	0.000	−0.089	0.045
	O	0.000	0.000	−0.012	0.000	0.000	−0.067	
NNO	N	0.000	0.000	−0.111	0.000	0.000	−0.146	0.254
	N	0.000	0.000	−0.125	0.000	0.000	0.038	
	O	0.000	0.000	0.150	0.000	0.000	0.447	
H_2CO	C	0.000	0.000	0.114	0.000	0.000	0.192	1.108
	O	0.000	0.000	0.132	0.000	0.000	0.302	
	H	0.113	0.000	0.075	0.086	0.000	0.109	
	H	−0.113	0.000	0.075	−0.086	0.000	0.109	
NH_3	N	0.000	0.000	0.231	0.000	0.000	0.032	0.598
	H	0.164	0.000	0.062	1.772	0.000	0.050	
	H	−0.082	−0.142	0.062	−0.886	−0.128	0.050	
	H	−0.082	0.142	0.062	−0.886	0.128	0.050	
H_2O	O	0.000	0.000	0.165	0.000	0.000	−0.021	0.730
	H	0.174	0.000	0.128	0.199	0.000	0.165	
	H	−0.174	0.000	0.128	−0.199	0.000	0.165	
HF	F	0.000	0.000	0.099	0.000	0.000	0.018	0.709
	H	0.000	0.000	0.258	0.000	0.000	0.334	
PH_3	P	0.000	0.000	0.168	0.000	0.000	−0.008	0.229
	H	0.097	0.000	0.049	−0.044	0.000	−0.026	
	H	−0.048	−0.084	0.049	0.022	0.038	−0.026	
	H	−0.048	0.084	0.049	0.022	−0.038	−0.026	
H_2S	S	0.000	0.000	0.037	0.000	0.000	0.020	0.402
	H	0.000	0.117	0.099	0.117	0.087	0.073	
	H	0.000	−0.117	0.099	−0.117	−0.087	0.073	
HCl	Cl	0.000	0.000	−0.020	0.000	0.000	0.008	0.451
	H	0.000	0.000	0.192	0.000	0.000	0.271	
SO_2	S	0.000	0.000	0.007	0.000	0.000	0.317	0.720
	O	0.000	−0.084	0.039	0.000	−0.532	0.159	
	O	0.000	0.084	0.039	0.000	0.532	0.159	

and

$$f^-(r) \approx \rho_N(r) - \rho_{N-1}(r) \tag{18}$$

where $\rho_{N+1}(r)$, $\rho_N(r)$ and $\rho_{N-1}(r)$ are the electron densities of the $N + 1$, N, and $N − 1$ electron system, respectively.

A condensed form of these functions has been proposed by Yang and Mortier,[48] yielding:

$$f_k^+ \approx q_k(N + 1) - q_k(N) \tag{19}$$

$$f_k^- \approx q_k(N) - q_k(N - 1) \tag{20}$$

where $q_k(N + 1)$, $q_k(N)$, and $q_k(N − 1)$ are the atomic populations of the atom k in the $N + 1$, N, and $N − 1$ electron system, respectively.

It was also shown that the Fukui functions (15) and (16) can be approximated by the LUMO and HOMO densities respectively, i.e.[49]

$$f^+(r) \approx \rho_{LUMO}(r) \tag{27}$$

$$f^-(r) \approx \rho_{HOMO}(r) \tag{28}$$

This Fukui function has been calculated in many articles, and has indeed been shown to be a very valuable tool in the description of molecular reactivity. The main advantage of these condensed

Fukui functions is the fact that they can be used very easily (i.e., site selectivity can easily be derived), whereas the interpretation of the local Fukui functions is in some cases less straightforward and more subtle. The main drawback of their usage is that an adequate condensation scheme has to be chosen (which cannot be done based on physical grounds but is usually based mainly on "personal perference"), and that, in some cases, site selectivity may change when using two different population analysis schemes. Therefore, it is worthwhile to check the present condensation scheme as it is based on the partitioning of the charge density into atoms bearing some well-defined physical meaning.

Applications where the Hirshfeld charges were used to yield condensed Fukui functions are scarce. Roy et al. used Hirshfeld charges to calculate condensed Fukui functions for substituted anilines to study the preferred site of protonation. Moreover, they argued that, in contrast with other charge partitioning techniques, the Hirshfeld charge partitioning produces non-negative Fukui function indexes.[50,51] Gilardoni et al. calculated the condensed Fukui function using numerical integration using the Becke partitioning of the three-dimensional space into atomic regions. They concluded that the condensed Fukui functions obtained in this way provided "useful chemical information," and that the results were much less basis set dependent than with the use of Mulliken charges.[52]

The condensed Fukui function based on the Hirshfeld partitioning scheme was calculated for a large series of molecules. In Table 4, the condensed Fukui function for a series of simple molecules undergoing an electrophilic attack are listed. These were also considered in our past work.[27] In addition, the density of the HOMO, an approximation to the Fukui function, was also integrated over the Hirshfeld atomic regions, giving rise to the entries in the last column. As can be seen, both the finite difference
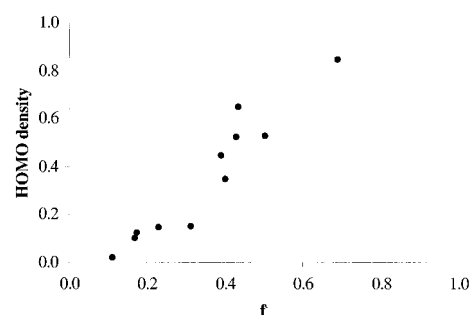

Figure 2. Correlation between the finite difference condensed Fukui function f^- and the integrated HOMO densities of CO, HCN, NNO, and H_2CO.

condensed Fukui function and the integrated HOMO density yield the correct selectivity for the molecules CO (attack on the carbon, in line with the fact that the HOMO for this molecule is a nonbonding σ orbital on this atom), H_2CO (electrophilic attack on the oxygen atom of the carbonyl group), HCN (attack on nitrogen), and NNO (attack on oxygen). As can be seen from these results, the selectivity between the two possible reaction sites decreases when orbital relaxation is introduced, going from the HOMO density to f^-. In Figure 2, the correlation between the finite difference Fukui function and the integrated HOMO density is plotted for these molecules. As can be seen, the agreement between both data sets can be considered as satisfactory.
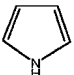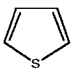
At the bottom of this table, the condensed Fukui functions and HOMO densities for three famous ambident nucleophiles are listed.[45,53–55] For the SCN^- molecule, the softest site is clearly the S, in agreement with experimental results.[55] For NO_2^- the results is somewhat more complex. The HOMO density predicts that N is the softest site within this molecule, in line with Klopman's analysis,[55] the softness difference between the two sites, however, being relatively small. With the condensed Fukui function, however, the oxygen becomes softer than nitrogen, in line with previous calculated condensed Fukui functions. In contrast with previous work however,[27] the softness difference between the two sites is much smaller, indicating that probably both atoms can be considered to be of more or less the same softness, and that a careful analysis of the local Fukui function is required. It was indeed shown by some of us that when considering the local Fukui function, the nitrogen is the softest atom in NO_2^-.[54] For the enolate ion, it is again clear that the electrophilic attack occurs on the carbon atom, as is found experimentally.[55] It is interesting to note that when AIM charges are used, the oxygen atom is the softest.[27]

In Table 5, selectivities (*ortho, meta,* and *para*) are shown for a classical organic chemistry textbook example, the electrophilic substitution on monosubstituted benzenes.[56] This reaction was previously studied by some of us using both soft and hard reactivity indices.[57,58] Condensed Fukui functions have been calculated, all based on the Mulliken population analysis. From this work, it has been concluded that the intramolecular reactivity sequences are predicted by the local softness (Fukui function), but that the intermolecular reactivity is best described by a hard index, such as, for example, the electrostatic potential.[58] Table 5 contains the condensed Fukui functions and integrated HOMO densities for

Table 4. Condensed Fukui Functions f^- and Integrated HOMO Densities for an Electrophilic Attack on a Number of Small Nucleophiles (All Values in $|e|$).

Molecule	Atom	f^-	HOMO
CO	C	0.687	0.845
	O	0.314	0.155
H_2CO	O	0.433	0.649
	C	0.229	0.147
	H	0.169	0.102
HCN	H	0.109	0.024
	C	0.389	0.447
	N	0.502	0.529
NNO	N	0.399	0.350
	N	0.173	0.124
	O	0.428	0.526
SCN^-	S	0.606	0.702
	C	0.115	0.082
	N	0.279	0.215
NO_2^-	N	0.310	0.372
	O	0.345	0.314
CH_2CO^-	C	0.324	0.467
	C	0.131	0.135
	O	0.273	0.296

Table 5. Condensed Fukui Functions and Integrated HOMO Densities for Monosubstituted Benzenes X-C$_6$H$_5$ (All Values in $|e|$).

X =	Site	f^-	HOMO	Exp.
NH$_3^+$	*o*	0.067	0.232	$p \geq m > o$
	m	0.095	0.195	
	p	0.175	0.034	
O$^-$	*o*	0.102	0.012	*o, p*
	m	0.057	0.064	
	p	0.136	0.003	
OH	*o*	0.091	0.124	$p \approx o > m$
		0.081	0.109	
	m	0.073	0.073	
		0.064	0.057	
	p	0.144	0.220	
NH$_2$	*o*	0.080	0.114	*o, p*
	m	0.061	0.050	
	p	0.131	0.186	
F	*o*	0.087	0.107	$p > o > m$
	m	0.078	0.083	
	p	0.158	0.252	
CHO	*o*	0.033	0.014	$m > o \gg p$
		0.044	0.012	
	m	0.045	0.005	
		0.044	0.004	
	p	0.072	0.001	
CH=CH$_2$	*o*	0.065	0.082	*o, p*
		0.059	0.089	
	m	0.054	0.041	
		0.059	0.050	
	p	0.115	0.158	
NO$_2$	*o*	0.118	0.211	$m \gg o > p$
	m	0.126	0.208	
	p	0.048	0.038	
	2	0.194	0.300	2
	3	0.068	0.140	
	2	0.272	0.298	2
	3	0.107	0.148	
	2	0.059	0.295	2
	3	0.138	0.139	

a series of eight monosubstituted benzenes and three heterocyclic rings—pyrrole, furan, and thiophene; in the last column, the experimentally found selectivity for the monosubstituted benzenes is listed, based on isomer distributions and partial rate factors. As can be seen, for the majority of cases, both the HOMO density and the Fukui function predict the correct reactivity sequence and give a good measure of the electronic effects caused by the substitutent. For the phenolate molecule, however, the HOMO density incorrectly predicts the most reactive site to be the *meta* position; when calculating the more general condensed Fukui function, however, this error is corrected and the *o* and *p* positions clearly appear as the preferred sites for electrophilic attack. In the case of nitrobenzene, a similar situation occurs. Based on the HOMO density, the *o* and *m* positions have a comparable reactiv-
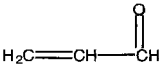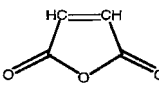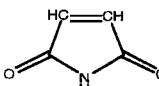
ity, with a slight preference for *o*, whereas the condensed Fukui function correctly predicts the *m* position as the most reactive one. The only problem occurs for X=CHO. As can be seen, the selectivity based on the HOMO orbital density is $o > m > p$. The condensed Fukui function only partially corrects this sequence: *m* becomes larger than *o*, but now *p* has an abnormally high Fukui function. It has to be mentioned, however, that in this molecule, the *m* carbon atoms bear the most negative charge: the *ortho* carbons have an average charge of -0.25, the meta carbons bear -0.35, whereas the *para* carbon has a charge of -0.23, thereby to a large extent recovering the experimental reactivity sequence.

At the bottom of this table, the aromatic heterocyclic five rings have been considered, pyrole, furan, and thiophene, where it is well known that the preferred site for the attack of a nucleophile are the carbons directly attached to the heteroatom. It can indeed be seen that this is recovered by considering both the HOMO density and the condensed Fukui function, except for the condensed Fukui function in thiophene. Again, however, the two carbons adjacent to the heteroatom have the largest negative charge compared to the two other ones, i.e., a charge of -0.07 for the former and -0.06 for the latter.

It has to be remarked, however, that these reactivity indices give information about the initial state or the onset of the reaction, so that, at least when the HOMO (or LUMO) densities are used, no information about the transition states and product distribution is present.

In Table 6, some examples are given for systems undergoing a nucleophilic attack. These consist of formaldehyde, acrolein, maleiimide, and maleic anhydride. Also listed in the same table is the value of the LUMO density integrated over the different Hirshfeld atoms. As can be seen, both the Fukui function and the LUMO density predict the correct site selectivity for a nucleophilic attack in the four molecules: the carbon atom in formaldehyde, the β-carbon in acrolein,[59] and the α-carbons in maleic anhydride and maleiimide.[52]

Table 6. Fukui Function Indices f^+ and Integrated LUMO Densities for Formaldehyde, Acrolein, Maleic Anhydride, and Maleiimide (All Values in $|e|$).

Molecule	Atom	f^+	LUMO
H$_2$CO	O	0.308	0.372
	C	0.397	0.518
	H	0.147	0.055
	C$_\beta$	0.211	0.291
	C$_\alpha$	0.116	0.157
	C$_{carb}$	0.171	0.239
	C$_{carb}$	0.097	0.130
	C	0.145	0.205
	C$_{carb}$	0.096	0.133
	C	0.137	0.194

Conclusions

Atomic charges, atomic dipole moments, and Fukui functions have been calculated using the Hirshfeld partitioning of the electron density. For a series of molecules containing functional groups frequently encountered in organic molecules, all expected bond polarities were recovered but the magnitudes are considerably smaller, in agreement with previously published works. In addition, the charge distributions in a series of so-called hypervalent compounds were investigated; upon comparison with the Hirshfeld charges of organic molecules and some ionic compounds, these could be classified as somewhat ionic. In a next part, correlated atomic dipoles were computed for a series of small molecules; moreover, the contributions of these atomic dipoles to the total molecular dipole moment were investigated, together with the contribution due to charge transfer. It could be concluded that the charge transfer term does in most cases not contain enough information to reproduce the total dipole moment of the molecule. Finally, Fukui function indices were calculated for a number of electrophiles and nucleophiles using the Hirshfeld charges. In addition, as an approximation to the Fukui function, the HOMO or LUMO density was integrated over the Hirshfeld atoms. In most cases, the integrated frontier MO and the Fukui function yield similar site selectivities; moreover, site selectivities were in the majority of cases in agreement with previous studies and with experiment. No negative Fukui function indices were encountered. On the whole, it can be concluded that the partitioning of the electron density due to Hirshfeld yields charges in agreement with chemical intuition, which can be considered as valuable tools to calculate Fukui function indices.

Acknowledgments

References

1. Bachrach, S. M. In Reviews of Computational Chemistry; Lipkowitz, W. B.; Boyd, D. B., Eds.; VCH: New York, 1995, p 171, vol. v.
2. Bader, R. F. W. Atoms in Molecules: A Quantum Theory; Oxford University Press: Oxford, 1990.
3. Nalewajski, R. F.; Parr, R. G. Proc Natl Acad Sci USA 2000, 97, 8879.
4. Mulliken, R. S. J Chem Phys 1955, 23, 1833, 1841, 2338, 2343.
5. Reed, A. E.; Weinstock, R. B.; Weinhold, F. J Chem Phys 1985, 83, 735.
6. Reed, A. E.; Weinhold, F. J Chem Phys 1985, 83, 1736.
7. Reed, A. E.; Curtiss, L. A.; Weinhold, F. Chem Rev 1988, 88, 899.
8. Singh, U. C.; Kollman, P. A. J Comp Chem 1984, 5, 129.
9. Breneman, C. M.; Wiberg, K. B. J Comput Chem 1990, 11, 361.
10. Cioslowski, J. J. Am Chem Soc 1989, 111, 8333.
11. Hirshfeld, F. L. Theor Chim Acta 1977, 44, 129.
12. Stewart, R. F. J Chem Phys 1965, 42, 3175.
13. Gill, P. M. W. J Phys Chem 1996, 100, 15421.
14. Maslen, E. N.; Spackman, M. A. Aust J Phys 1985, 38, 273.
15. Davidson, E. R.; Chakravorty, S. Theor Chim Acta 1992, 83, 319.
16. Wiberg, K. B.; Rablen, P. R. J Comput Chem 1993, 14, 1504.
17. Wiberg, K.; Castejon, H. J. Org Chem 1995, 60, 6327.
18. Wiberg, K. B.; Rablen, P. R. J Am Chem Soc 1995, 117, 2201.
19. Rousseau, B.; Peeters, A.; Van Alsenoy, C. Chem Phys Lett 2000, 324, 189.
20. De Proft, F.; Martin, J. M. L.; Geerlings, P. Chem Phys Lett 1996, 250, 393.
21. Rousseau, B.; Peeters, A.; Van Alsenoy, C. J Mol Struct (Theochem) 2001, 538, 235.
22. Becke, A. D. J Chem Phys 1993, 98, 5648.
23. Lee, C. T.; Yang, W. T.; Parr, R. G. Phys Rev B 1988, 37, 785.
24. Frisch, M. J.; Trucks, G. W.; Schlegel, H. B.; Scuseria, G. E.; Robb, M. A.; Cheeseman, J. R.; Zakrzewski, V. G.; Montgomery, J. A.; Stratmann, R. E.; Burant, J. C.; Dapprich, S.; Millam, J. M.; Daniels, A. D.; Kudin, K. N.; Strain, M. C.; Farkas, O.; Tomasi, J.; Barone, V.; Cossi, M.; Cammi, R.; Mennucci, B.; Pomelli, C.; Adamo, C.; Clifford, S.; Ochterski, J.; Petersson, G. A.; Ayala, P. Y.; Cui, Q.; Morokuma, K.; Malick, D. K.; Rabuck, A. D.; Raghavachari, K.; Foresman, J. B.; Cioslowski, J.; Ortiz, J. V.; Baboul, A. G.; Stefanov, B. B.; Liu, G.; Liashenko, A.; Piskorz, P.; Komaromi, I.; Gomperts, R.; Martin, R. L.; Fox, D. J.; Keith, T.; Al-Laham, M. A.; Peng, C. Y.; Nanayakkara, A.; Gonzalez, C.; Challacombe, M.; Gill, P. M. W.; Johnson, B.; Chen, W.; Wong, M. W.; Andres, J. L.; Gonzalez, C.; Head–Gordon, M.; Replogle, E. S.; Pople, J. A. Gaussian 98, Revision A7; Gaussian Inc.: Pittsburgh, PA, 1998.
25. Hehre, W. J.; Radom, L.; Schleyer, P. v. R.; Pople, J. A. Ab Initio Molecular Orbital Theory; Wiley: New York, 1986.
26. Geerlings, P.; De Proft, F.; Martin, J. M. L. In Recent Developments in Density Functional Theory; Seminario, J. M., Ed.; Elsevier: Amsterdam, 1996, p. 773.
27. De Proft, F.; Martin, J. M. L.; Geerlings, P. Chem Phys Lett 1996, 256, 400.
28. De Proft, F.; Geerlings, P. J Chem Phys 1997, 106, 3270.
29. Geerlings, P.; De Proft, F.; Langenaeker, W. Adv Quant Chem 1999, 33, 303.
30. Koch, W.; Holthausen, M. C. A Chemist's Guide to Density Functional Theory; Wiley–VCH: Weinheim, 2000.
31. Pople, J. A.; Head–Gordon, M.; Raghavachari, K. J Chem Phys 1987, 87, 5968.
32. Dunning, T. H. J. Chem Phys 1989, 90, 1007.
33. Kendall, R. A.; Dunning, T. H.; Harrison, R. J. J Chem Phys 1992, 96, 6796.
34. Becke, A. D. J Chem Phys 1988, 88, 2547.
35. Murray, C. W.; Handy, N. C.; Laming, G. J. Mol Phys 1993, 78, 997.
36. Lebedev, V. I.; Skorokhodov, A. L. Russian Acad Sci Dokl Math 1992, 45, 587.
37. Gill, P. M. W.; Johnson, B. G.; Pople, J. A. Chem Phys Lett 1993, 209, 506.
38. Stratmann, R. E.; Scuseria, G. E.; Frisch, M. J. Chem Phys Lett 1996, 257, 213.
39. Reed, A. E.; Schleyer, P. V. J Am Chem Soc 1990, 112, 1434.
40. Figeys, H. P.; Geerlings, P.; Van Alsenoy, C. J. Chem Soc Faraday Trans II 1979, 75, 528.
41. Figeys, H. P.; Geerlings, P.; Van Alsenoy, C. J. Chem Soc Faraday Trans II 1979, 75, 542.
42. Figeys, H. P.; Geerlings, P.; Theoretical Models of Chemical Bonding, Part 3; Maksic, Z. B., Eds.; Springer-Verlag: Berlin-Heidelberg, 1991, p 25, vol 3.

43. Parr, R. G.; Yang, W. T. J Am Chem Soc 1984, 106, 4049.
44. Fukui, K.; Yonezawa, T.; Shinghu, H. J Chem Phys 1972, 20, 722.
45. Parr, R. G.; Yang, W. Density-Functional Theory of Atoms and Molecules; Oxford University Press: Oxford, 1989.
46. Parr, R. G.; Yang, W. Annu Rev Phys Chem 1995, 46, 701.
47. Kohn, W.; Becke, A. D.; Parr, R. G. J Phys Chem 1996, 100, 12974.
48. Yang, W.; Mortier, W. J. J Am Chem Soc 1986, 108, 5708.
49. Yang, W.; Parr, R. G.; Pucci, R. J Chem Phys 1984, 81, 2862.
50. Roy, R. K.; Pal, S.; Hirao, K. J Chem Phys 1999, 110, 8236.
51. Roy, R. K.; Hirao, K.; Pal, S. J Chem Phys 2000, 113, 1372.
52. Gilardoni, F.; Weber, J.; Chermette, H.; Ward, T. R. J Phys Chem A 1998, 102, 3607.
53. Lee, C.; Yang, W.; Parr, R. G. J Mol Struct (Theochem) 1988, 163, 305.
54. Langenaeker, W.; De Proft, F.; Geerlings, P. J Mol Struct (Theochem) 1996, 362, 175.
55. Klopman, G. Chemical Reactivity and Reaction Paths; Wiley: New York, 1974.
56. Taylor, R. Electrophilic Aromatic Substitution; Wiley: New York, 1990.
57. Langenaeker, W.; Demel, K.; Geerlings, P. J Mol Struct (Theochem) 1991, 234, 329.
58. Langenaeker, W.; De Proft, F.; Geerlings, P. J Phys Chem 1995, 99, 6424.
59. Langenaeker, W.; Demel, K.; Geerlings, P. J Mol Struct (Theochem) 1992, 259, 317.